

**Phosphite-containing iridium polarization transfer catalysts
for NMR signal amplification by reversible exchange**

**Kirill A. Spiridonov, Vitaly P. Kozinenko, Igor A. Nikovsky,
Alexander A. Pavlov, Tatyana N. Vol'khina, Yulia V. Nelyubina,
Alexey S. Kiryutin, Alexandra V. Yurkovskaya, Alexander A. Polezhaev,
Valentin V. Novikov and Konstantin L. Ivanov[†]**

Table of contents

Synthetic procedures

Parahydrogen experiments

Supplementary references

Supplementary figures

[†] Deceased.

Synthesis. All synthetic manipulations were carried out under an atmosphere of purified argon. All solvents were refluxed and distilled over appropriate reagents under argon atmosphere. Deuterated solvents were carefully dried by known procedures and stored under argon prior to use. The starting complexes [IrCl(COD)(SIMes)] and [IrCl(COD)(SIPr)] were prepared following the reported approaches [S1]. Imidazolium salts SIMes·HCl (1,3-bis-(2,4,6-trimethylphenyl)imidazolium chloride) and SIPr·HCl (1,3-bis(2,6-diisopropylphenyl)imidazolium chloride) were purchased from Aldrich. Commercial reagents were used as received without further purification. The NMR spectra were recorded on Bruker Avance 400 and Bruker Avance III 700 MHz spectrometers. Elemental analysis was performed using an automatic C,H,N analyzer.

[IrCl(COD)(SIPr)] ([1,3-bis[2,6-diisopropylphenyl]-2-imidazolidinylidene]chloro[η^4]-1,5-cyclooctadiene]iridium): In a flame-dried Schlenk tube, η^4 -cycloocta-1,5-diene iridium(I) chloride dimer [Ir(Cl)(COD)]₂ (537 mg, 0.80 mmol) and Bu^tOK (80 mg, 0.80 mmol) were mixed and stirred under high vacuum for 10 min. Then, dry THF (10 mL) was added under an argon atmosphere, and the resulting red-black solution was stirred at r.t. for other 10 min. Subsequently, imidazolium salt SIPr HCl (680 mg, 1.60 mmol) was added in one portion causing a change of color from dark red to dark yellow, and the reaction mixture was stirred for 16 h. The THF was then removed in vacuo, and the residue was purified by flash column chromatography, eluting a yellow fraction with a 1:1 mixture of EtOAc and petroleum ether. Yield: 904 mg (78%). ¹H NMR (400 MHz, CDCl₃): δ = 7.45 (t, ³J_{H-H} = 7.7 Hz, 2H, ArH), 7.36-7.29 (m, 4H, ArH), 7.00 (s, 2H, ArH), 4.19-4.16 (m, 2H, COD CH), 3.47-3.37 (m, 2H, CH(CH₃)₂), 2.88-2.86 (m, 2H, COD CH), 2.73-2.64 (m, 2H, CH(CH₃)₂), 1.71-1.62 (m, 2H, COD CH₂), 1.54-1.11 (m, 16H, COD CH₂ and CH(CH₃)₂), 1.08 (d, J = 6.7 Hz, 12H, CH(CH₃)₂), 0.93-0.81 (m, 2H, COD CH₂). ¹³C NMR (100 MHz, CDCl₃): δ = 181.9, 135.7, 129.2, 123.8, 122.4, 82.3, 50.9, 33.0, 28.4, 28.2, 25.9, 22.7, 22.0.

[IrCl(COD)(SIMes)] ([1,3-bis[2,4,6-trimethylphenyl]-2-imidazolidinylidene]chloro[η^4]-1,5-cyclooctadiene]iridium): In a flame-dried Schlenk tube, η^4 -cycloocta-1,5-dieneiridium(I) chloride dimer [Ir(Cl)(COD)]₂ (537 mg, 0.80 mmol) and Bu^tOK (80 mg, 0.80 mmol) were mixed and stirred under high vacuum for 10 min. Then, dry THF (10 mL) was added under an argon atmosphere, and the resulting red-black solution was stirred at r.t. for other 10 min. Subsequently, the dihydroimidazol-2-ylidene SIMes HCl (544 mg, 1.60 mmol) was added in one portion causing a change of color from dark red to dark yellow, and the reaction mixture was stirred for 16 h. The THF was then removed in vacuo, and the residue was purified by

flash column chromatography, eluting a yellow fraction with a 8:1 mixture of dichloromethane and acetone as eluent. Yield: 875 mg (86%). ^1H NMR (400 MHz, CDCl_3): δ 7.30 (t, 2H, $^3J_{\text{H-H}} = 7.5$ Hz, ArH), 7.21 -7.17 (m, 4H, ArH), 7.01 (s, 2H, NCH=CHN), 4.18-4.13 (m, 2H, COD CH), 2.98-2.93 (m, 2H, COD CH), 2.41 (s, 6H, ArCH₃), 2.22 (s, 6H, ArCH₃), 1.75-1.59 (m, 4H, COD CH₂), 1.38-1.31 (m, 2H, COD CH₂), 1.27-1.21 (m, 2H, COD CH₂). ^{13}C NMR (100 MHz, CDCl_3): δ 179.6, 137.4, 136.8, 133.8, 128.0, 127.8, 126.5, 122.2, 81.9, 50.5, 32.5, 27.9, 18.8, 17.3.

[Ir(COD){PO(Ph)₃}(SIMes)]BF₄ ([1,3-bis[2,4,6-trimethylphenyl]-2-imidazolidinylidene] [(η^4)-1,5-cyclooctadiene](triphenyl phosphite)iridium tetrafluoroborate, **1**): A solution of [IrCl(COD)(SIMes)] (592 mg, 0.93 mmol) in acetone (10 mL) was treated with 1 equiv of AgBF₄ (181 mg, 0.93 mmol) and stirred in the dark at room temperature for 30 min. The resulting suspension was filtered through Celite and evaporated to dryness. The obtained residue was re-dissolved in THF (10 mL), and triphenyl phosphite (0.268 mL, 1.02 mmol) was added to produce a mixture that was then stirred at room temperature for 1 h and concentrated to ca. 1 mL. Addition of diethyl ether gave an orange solid, which was separated by decantation, washed with diethyl ether and dried *in vacuo*. Yield: 649 mg (86%). ^1H NMR (600 MHz, CD_2Cl_2 , 20 °C), δ (ppm): 0.84 (m, 2H, CH₂(COD)), 1.1–1.5 (m, 6H, CH₂(COD)), 1.13 (d, $^3J_{\text{HH}} = 2.3$ Hz, 3H, Me), 1.14 (d, $^3J_{\text{HH}} = 2.3$ Hz, 3H, Me), 1.18 (d, $^3J_{\text{HH}} = 2.3$ Hz, 3H, Me), 1.20 (d, $^3J_{\text{HH}} = 2.3$ Hz, 3H, Me), 1.30 (d, $^3J_{\text{HH}} = 2.3$ Hz, 3H, Me), 1.31 (d, $^3J_{\text{HH}} = 2.3$ Hz, 3H, Me), 1.49 (d, $^3J_{\text{HH}} = 2.3$ Hz, 3H, Me), 1.50 (d, $^3J_{\text{HH}} = 2.3$ Hz, 3H, Me), 3.18 (m, 2H, CH(*i*-Pr)), 3.68 (m, 2H, N-CH₂), 3.79 (m, 2H, CH(*i*-Pr)), 4.32 (m, 2H, CH(COD)), 4.47 (m, 2H, CH(COD)), 5.03 (m, 2H, N-CH₂), 6.82 (m, 6H, *m*-Ph), 7.18 (m, 9H, *o*-Ph, *p*-Ph), 7.35 (m, 2H, *m*-H(SIPr)), 7.43 (m, 2H, *m*-H(SIPr)), 7.54 (m, 2H, *p*-H(SIPr)). $^{31}\text{P}\{^1\text{H}\}$ NMR (162 MHz, CD_2Cl_2 , 20 °C), δ (ppm): 88.02 (s). $^{13}\text{C}\{^1\text{H}\}$ NMR (150 MHz, CDCl_3 , 25 °C), δ (ppm): 22.45, 23.02 (all s, CH(*i*-Pr)), 28.02, 28.15, 28.85, 29.77 (all s, Me), 29.91, 30.59 (all s, CH₂(COD)), 55.61 (s, CH(COD)), 77.99 (s, N-CH₂), 90.51 (d, $^4J_{\text{CP}} = 17$ Hz, N-CH₂), 120.93 (d, $^4J_{\text{CP}} = 4$ Hz, *m*-Ph), 124.48, 125.34 (all s, *o*-SIPr), 125.76 (s, *p*-SIPr), 129.89 (s, *o*-Ph), 130.43 (s, *p*-Ph), 136.09 (s, *i*-SIPr), 146.43, 149.16 (all s, *o*-SIPr), 151.40 (d, $^2J_{\text{CP}} = 14$ Hz, *i*-Ph), 205.20 (d, $^2J_{\text{CP}} = 10$ Hz, C=Ir). NMR spectra are shown in Figures S5-S7. Anal. Calc. for (C₄₉H₅₇IrN₂O₃P): C, 62.27, H, 6.08, N, 2.96; Found: C, 62.35, H, 6.13, N, 2.99.

[Ir(COD){PO(Ph)₃}(SIPr)]BF₄ ([1,3-bis[2,6-diisopropylphenyl]-2-imidazolidinylidene] [(η^4)-1,5-cyclooctadiene](triphenyl phosphite)iridium tetrafluoroborate, **2**): A solution of [IrCl(COD)(SIPr)] (600 mg, 0.82 mmol) in acetone (10 mL) was treated with 1 equiv of AgBF₄ (159 mg, 0.82 mmol) and stirred in the dark at room temperature for 30 min. The

resulting suspension was filtered through Celite and evaporated to dryness. The obtained residue was re-dissolved in THF (10 mL), and triphenyl phosphite (0.236 mL, 0.90 mmol) was added to produce a mixture that was stirred at room temperature for 1 h and concentrated to ca. 1 mL. Addition of diethyl ether gave an orange solid, which was separated by decantation, washed with diethyl ether and dried *in vacuo*. Yield: 649 mg (86%). ^1H NMR (400 MHz, CD_2Cl_2 , 20 °C), δ (ppm): 0.9–1.1 (m, 4H, $\text{CH}_2(\text{COD})$), 1.15–1.3 (m, 4H, $\text{CH}_2(\text{COD})$), 2.43 (s, 12H, *o*-Me), 2.63 (s, 6H, *p*-Me), 3.75 (m, 2H, N- CH_2), 4.07 (m, 2H, CH(COD)), 4.13 (m, 2H, CH(COD)), 4.83 (m, 2H, N- CH_2), 6.75 (m, 6H, *m*-Ph), 7.16 (m, 13H, *o*-Ph, *p*-Ph, *m*-H(SIMes)). $^{31}\text{P}\{^1\text{H}\}$ NMR (162 MHz, CD_2Cl_2 , 20 °C), δ (ppm): 93.69 (s). $^{13}\text{C}\{^1\text{H}\}$ NMR (150 MHz, CD_2Cl_2 , 20 °C), δ (ppm): 18.42, 18.71, 20.85 (all s, Me), 30.03, 31.21 (all s, $\text{CH}_2(\text{COD})$), 52.80 (s, CH(COD)), 80.74 (s, N- CH_2), 87.82 (d, $^4J_{\text{CP}} = 18$ Hz, N- CH_2), 120.72 (d, $^4J_{\text{CP}} = 4$ Hz, *m*-Ph), 125.51 (s, *m*-SIMes), 129.77 (s, *p*-Ph), 129.96 (d, $^3J_{\text{CP}} = 9$ Hz, *o*-Ph), 134.34 (s, *i*-SIMes), 136.16 (s, *o*-SIMes), 137.20 (s, *p*-SIMes), 139.75 (s, *o*-SIMes), 150.95 (d, $^2J_{\text{CP}} = 12$ Hz, *i*-Ph), 199.59 (d, $^2J_{\text{CP}} = 10$ Hz, C=Ir). NMR spectra are shown in **Figs. S8-10**. Anal. Calc. for ($\text{C}_{55}\text{H}_{69}\text{IrN}_2\text{O}_3\text{P}$): C, 64.18, H, 6.76, N, 2.72; Found: C, 64.24, H, 6.69, N, 2.71.

Experiments with parahydrogen. NMR experiments with parahydrogen were performed using a Bruker Avance III 400 MHz spectrometer. Dihydrogen gas was enriched to 95% in its para component in a helium cryostat CFA-200-H2CELL (CryoPribor). To create hyperpolarization in a controlled and reproducible manner, we used an automatized gas bubbling setup [S2] that allowed us to bubble parahydrogen (here bubbling was performed at a pressure of 5 bar). The temperature in all the experiments was set to 25 °C. To analyze the process of catalyst activation, we performed a set of repetitive experiments, with each experiment containing the following stages: (1) 5 s of parahydrogen bubbling, (2) 1 s delay to stabilize the solution after the bubbling process, (3) detection of ^1H NMR spectrum with a 45-degree hard radiofrequency (RF) pulse, (4) 2 s relaxation delay. The described set included 64 experiments, resulting in 320 s of parahydrogen bubbling in total. The RF-pulse flip angle was set to 45 degrees to track both the spin polarization and the two-spin order.

Experiments at low and ultralow fields were performed with a shuttling device [S3] designed to transport the sample between a low (or even ultralow) polarization and high detection field of 9.4 T. In such experiments, the transfer of parahydrogen spin order to the substrate occurred at a variable polarization field B_{pol} . Subsequent transfer of the sample to the high field of the spectrometer allowed us to detect high resolution ^1H and ^{15}N spectra. To

gain the highest signal enhancement, we have measured its dependence on the external magnetic field B_{pol} (Figure S3).

The ^1H NMR enhancements have been determined by comparing the signal intensities in the corresponding SABRE spectra to those in thermal NMR spectra. To estimate the ^{15}N signal enhancement, a different strategy was used, as the signals in the corresponding thermal NMR spectrum had extremely low intensity. Thereby, we have obtained the ^{15}N NMR spectrum for a reference sample with the same concentration of ^{15}N -labeled pyridine and compared the signal intensities in this spectrum to those in the SABRE spectra.

Supplementary references

- [S1]. W. J. Kerr, M. Reid and T. Tuttle, *ACS Catal.*, 2015, **5**, 402.
- [S2]. A. S. Kiryutin, G. Sauer, S. Hadjiali, A. V. Yurkovskaya, H. Breitzke and G. Buntkowsky, *J. Magn. Reson.*, 2017, **285**, 26.
- [S3]. I. V. Zhukov, A. S. Kiryutin, A. V. Yurkovskaya, Y. A. Grishin, H.-M. Vieth and K. L. Ivanov, *Phys. Chem. Chem. Phys.*, 2018, **20**, 12396.

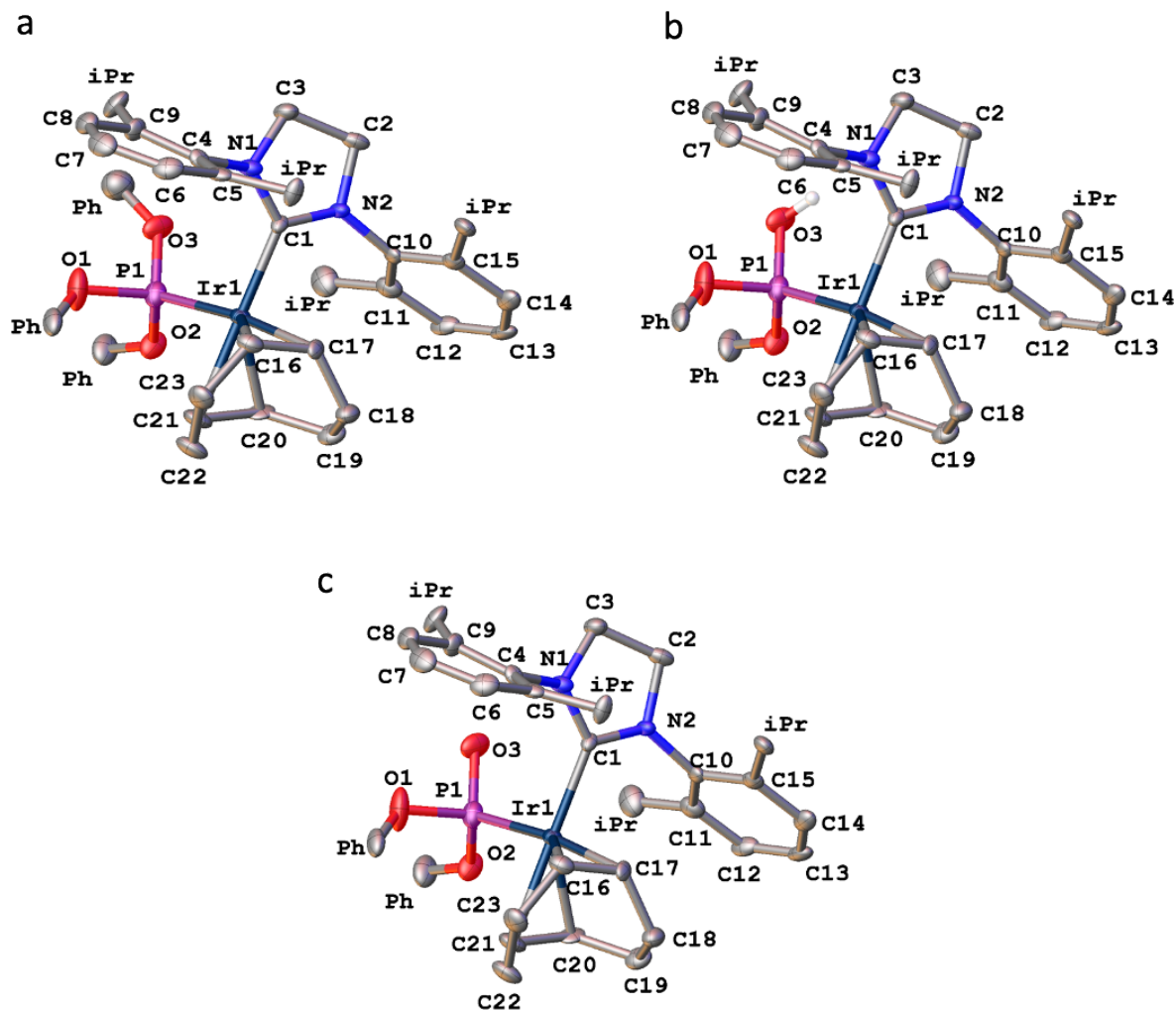


Figure S1 General view of the complex $[\text{Ir}(\text{COD})\text{P}(\text{OPh})_3(\text{SIPr})][\text{BF}_4]$ (a) and its two side-products, $[\text{Ir}(\text{COD})\text{P}(\text{OPh})_2(\text{OH})(\text{SIPr})][\text{BF}_4]$ (b) and $[\text{Ir}(\text{COD})\text{P}(\text{OPh})_2(\text{O})(\text{SIPr})]$ (c), identified by X-ray diffraction to coexist in the crystal of **2** in a 3:1:4 ratio. Hydrogen atoms except those of the OH group, tetrafluoroborate anions and disordered solvent molecules (modelled explicitly or treated as a diffuse contribution to the overall scattering) are omitted for clarity. Other atoms are shown as thermal ellipsoids at 50% probability level; **Ph** and **Pr**¹ stand for phenyl and isopropyl groups, respectively. The co-existence of the complexes $[\text{Ir}(\text{COD})\text{P}(\text{OPh})_2(\text{OH})(\text{SIPr})][\text{BF}_4]$ and $[\text{Ir}(\text{COD})\text{P}(\text{OPh})_2(\text{O})(\text{SIPr})]$ with the target product $[\text{Ir}(\text{COD})\text{P}(\text{OPh})_3(\text{SIPr})][\text{BF}_4]$ was supported by one of the three P-O bonds (av. 1.575 Å) being shorter than the others (av. 1.590 Å), which are typical of Ir-P(OX)₃ bonding (see above). There is also a pronounced difference between the above mean value of 2.250 Å and the bond lengths Ir-P in two symmetry independent species (2.207(3) and 2.236(2) Å), which are time- and space-averages of $[\text{Ir}(\text{COD})\text{P}(\text{OPh})_3(\text{SIPr})][\text{BF}_4]$ and $[\text{Ir}(\text{COD})\text{P}(\text{OPh})_2(\text{OH})(\text{SIPr})][\text{BF}_4]$ and of those two complexes with $[\text{Ir}(\text{COD})\text{P}(\text{OPh})_2(\text{O})(\text{SIPr})]$, respectively. An observed difference can be explained by a smaller contribution of the complex with three bulky phenyl groups, $[\text{Ir}(\text{COD})\text{P}(\text{OPh})_3(\text{SIPr})][\text{BF}_4]$, in the case of the independent moiety with a shorter Ir-P bond (2.207(3) vs. 2.236(2) Å). Besides, its average length (2.222 Å) is rather close to the quoted mean value for the iridium complexes with an IrP(OX)₃ moiety. In contrast, the Ir-C bonds to both the ligands SIPr (2.058(9) vs. 2.063(8) Å) and COD (av. 2.21 vs. 2.21 Å) are the same within the accuracy of the measurement and are very similar to those in the corresponding iridium complexes from Cambridge Structural Database.

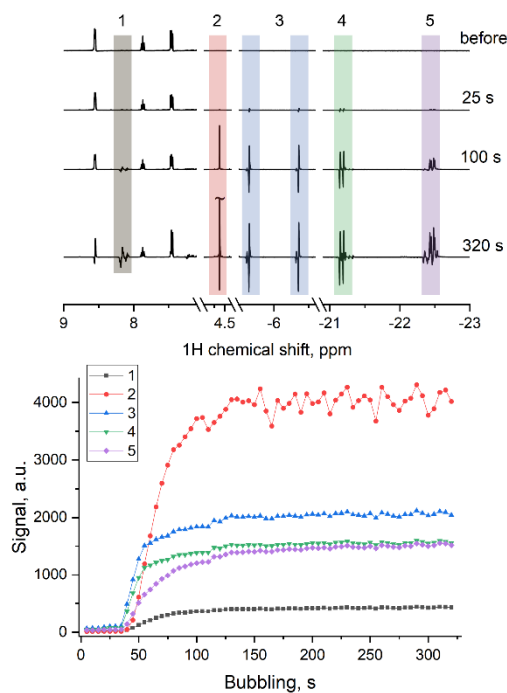


Figure S2 Polarization transfer from the parahydrogen molecule to the complex **1**. Top: 400 MHz NMR spectra obtained by a $\pi/4$ pulse before bubbling parahydrogen through a 2 mM methanol- d_4 solution of **1** in the presence 40 mM pyridine and after 25, 100 and 320 seconds of bubbling. Bottom: integral intensity of the selected signals vs. time of parahydrogen bubbling. Assignments: 1 – ortho-proton of the coordinated pyridine species, 2 – orthohydrogen, 3 – hydride complex after the dissociation of the phosphite moiety, 4 and 5 – hydride complexes with a different number of coordinated methanol and pyridine species.

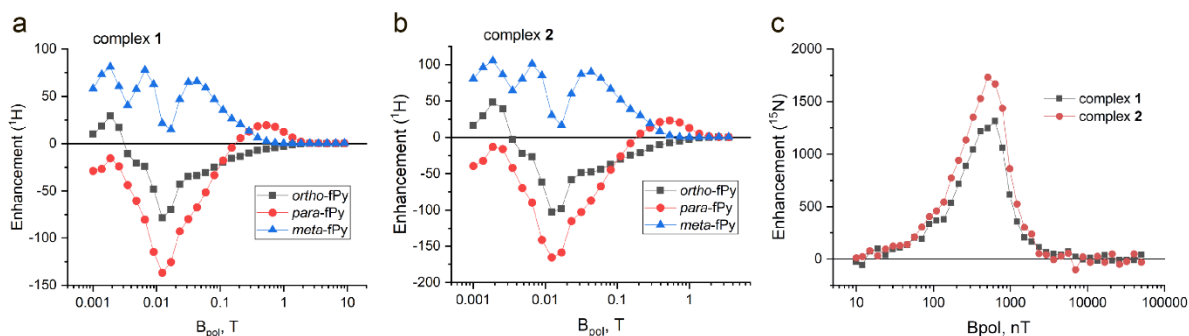


Figure S3 Field dependence of the ¹H NMR signal enhancements in free pyridine (shown here for the ortho-, meta- and para-protons) observed in the SABRE experiments with the complex **1** (a) and the complex **2** (b), and the field dependence of the ¹⁵N NMR signal enhancement of free pyridine for both these complexes (c).

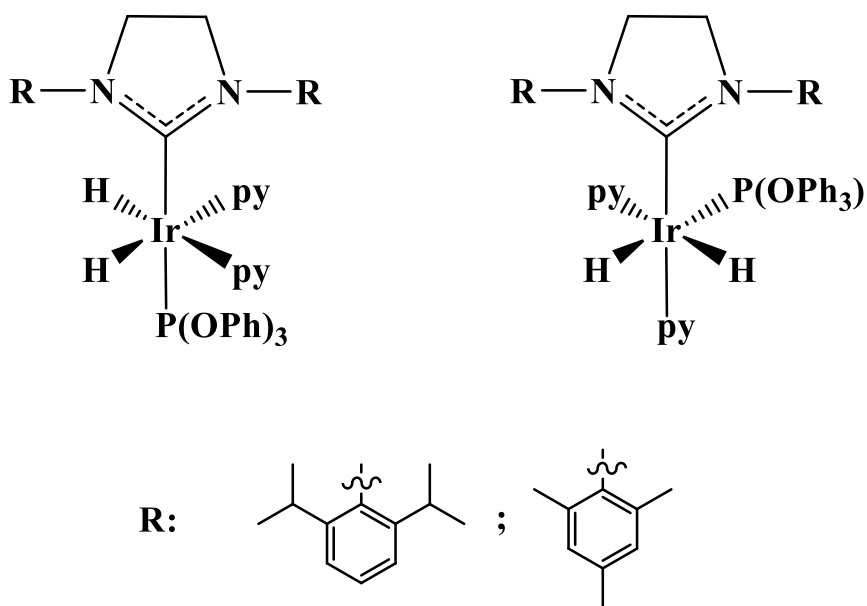


Figure S4. Possible hydride complexes formed during bubbling parahydrogen through a methanol- d_4 solution of the obtained complexes in the presence of pyridine.

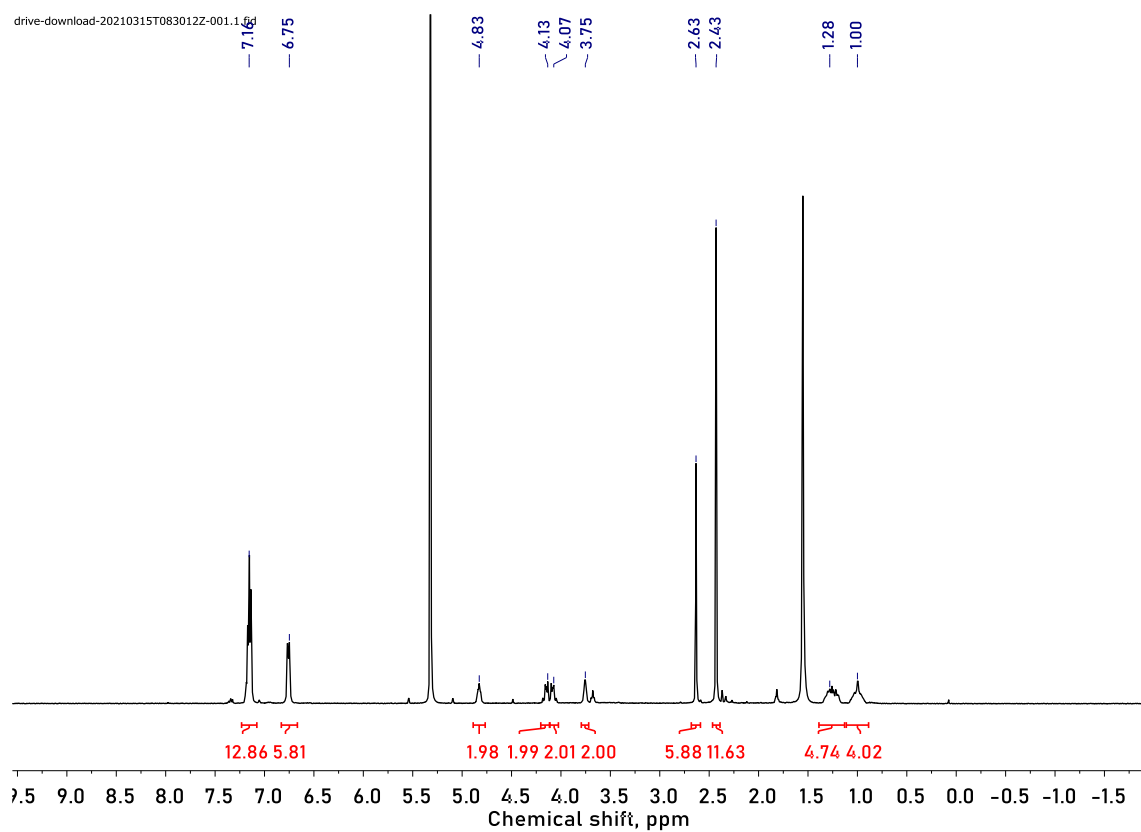


Figure S5. ^1H NMR spectrum (400 MHz, CD_2Cl_2 , 20 $^\circ\text{C}$) of complex **1**.

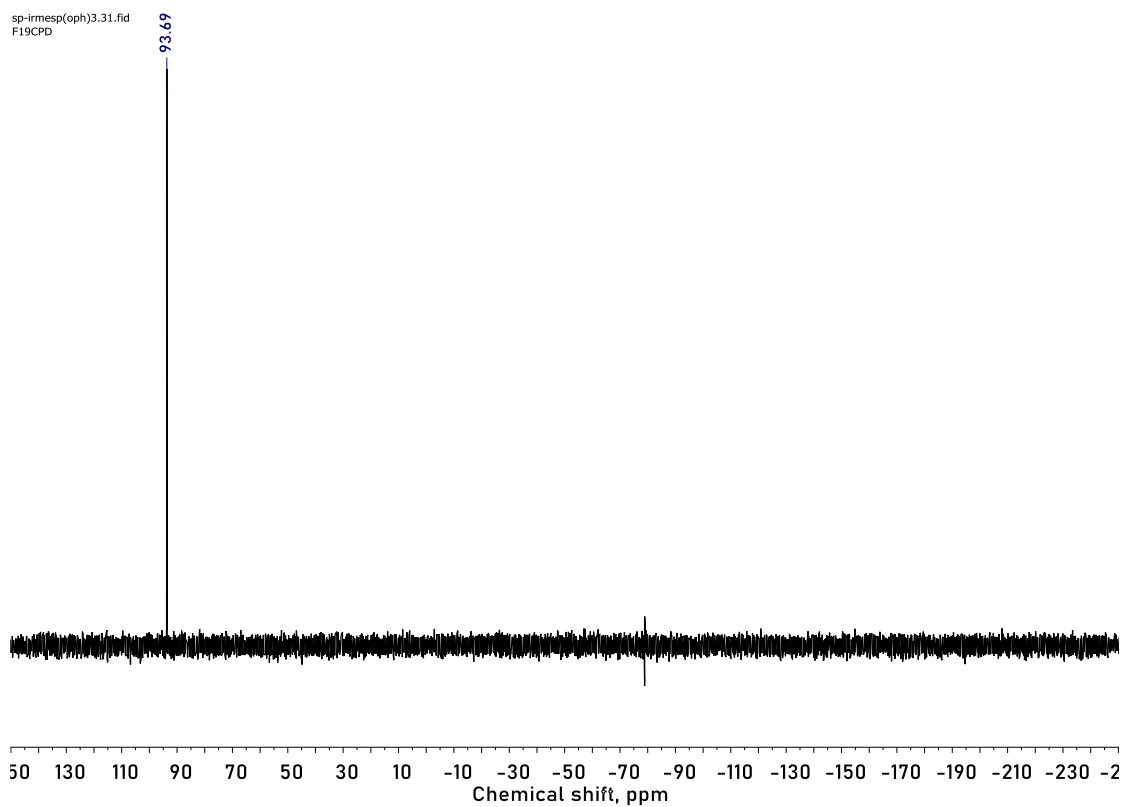


Figure S6. $^{31}\text{P}\{^1\text{H}\}$ NMR spectrum (162 MHz, CD_2Cl_2 , 20 °C) of complex **1**.

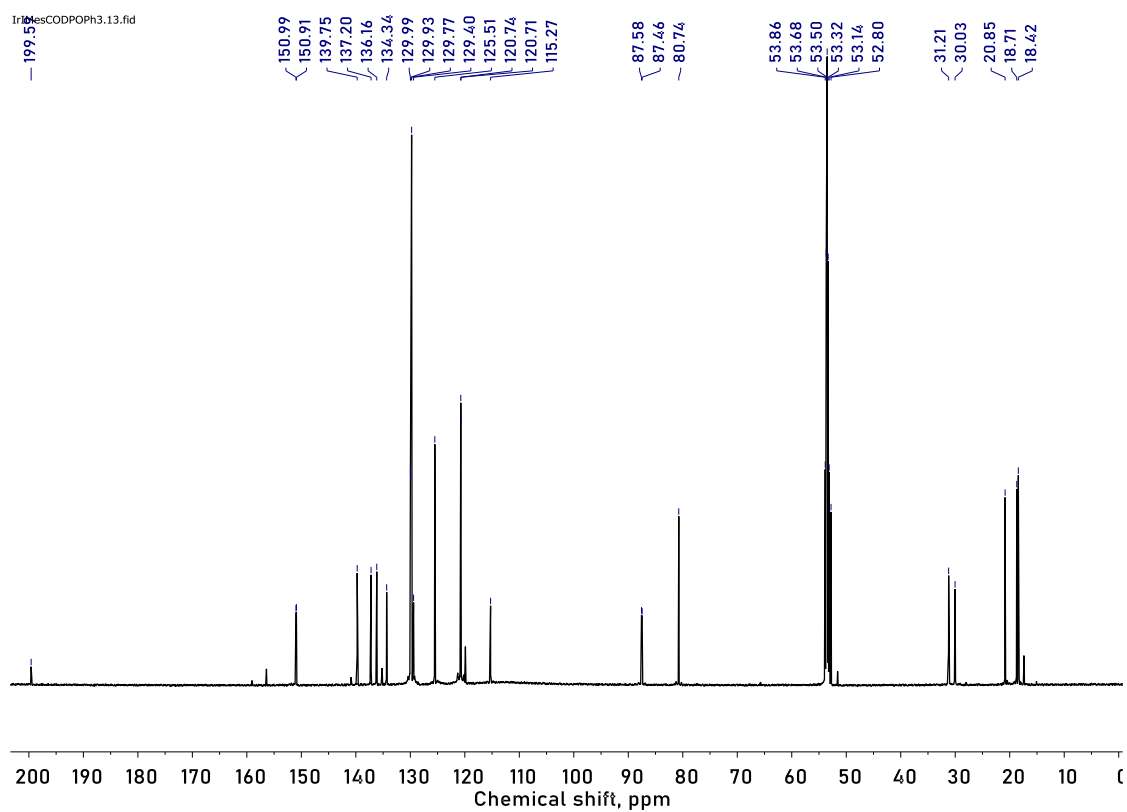


Figure S7. $^{13}\text{C}\{^1\text{H}\}$ NMR spectrum (150 MHz, CD_2Cl_2 , 20 °C) of complex **1**.

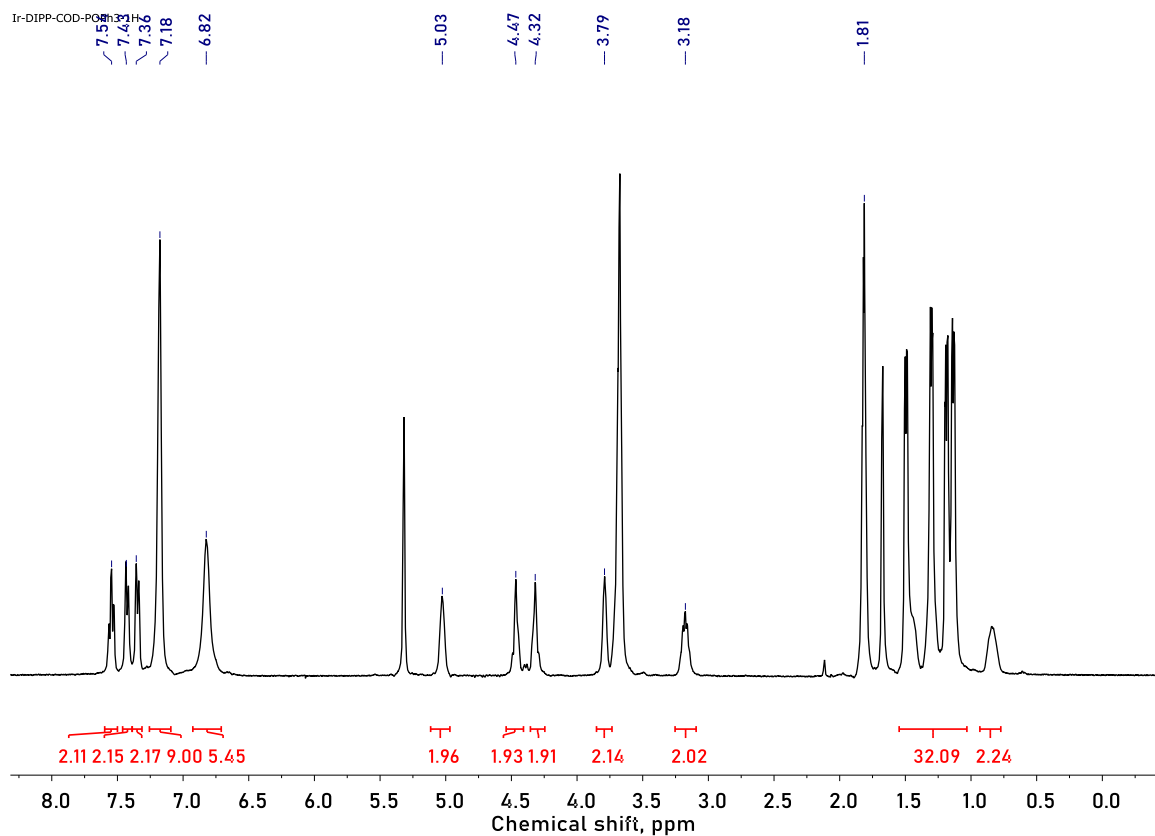


Figure S8. ^1H NMR spectrum (600 MHz, CD_2Cl_2 , 20 °C) of complex **2**.

Ir-DIPP-COD-POPPh3-31P
STANDARD PHOSPHORUS PARAMETERS

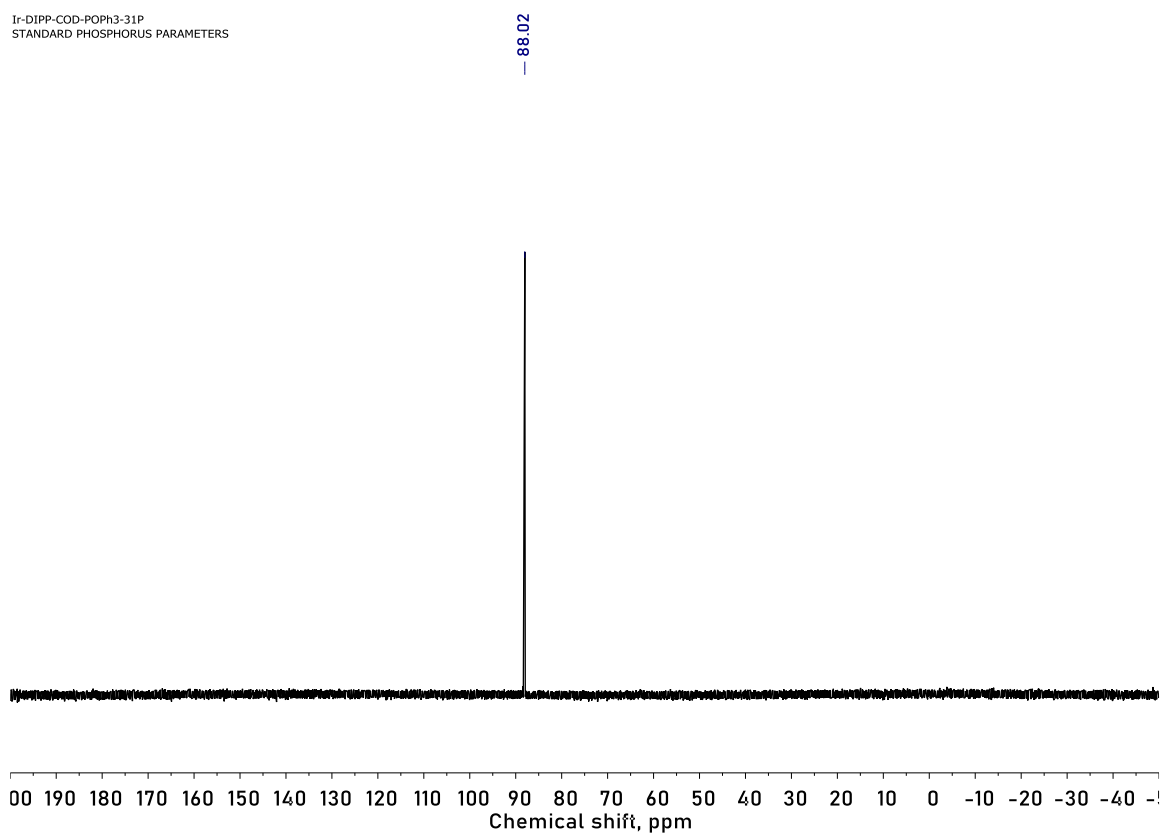


Figure S9. $^{31}\text{P}\{^1\text{H}\}$ NMR spectrum (162 MHz, CD_2Cl_2 , 20 °C) of complex **2**.

KV_20250222_SABRE_Cat2.3.fid
13C zg 300.13 600 mkl + Cat 24.7 mg
T = 25

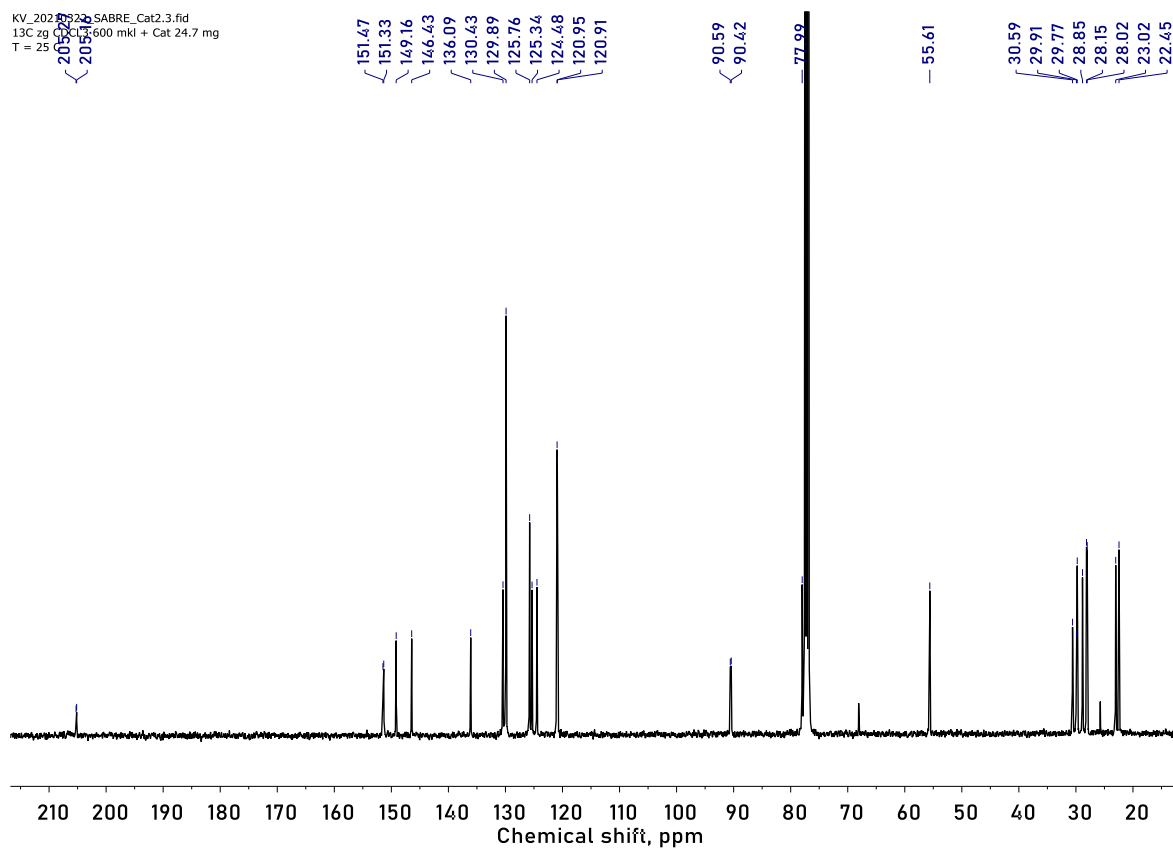


Figure S10. $^{13}\text{C}\{^1\text{H}\}$ NMR spectrum (162 MHz, CDCl_3 , 20 °C) of complex **2**.